LIPID DIFFUSIBILITY IN THE INTACT ERYTHROCYTE MEMBRANE

JOHN A. BLOOM AND WATT W. WEBB
Department of Physics and School of Applied and Engineering Physics, Clark Hall, Cornell University, Ithaca, New York 14853

ABSTRACT The lateral diffusion of fluorescent lipid analogues in the plasma membrane of intact erythrocytes from man, mouse, rabbit, and frog has been measured by fluorescence photobleaching recovery (FPR). Intact cells from dystrophic, normoblastic, hemolytic, and spherocytotic mouse mutants; from hypercholesterolemic rabbits and humans; and from prenatal, neonatal, and juvenile mice have been compared with corresponding normals. The lateral diffusion coefficient (D) for 3,3'-dioctadecylindodicarbocyanine iodide (DiI[5]) in intact normal human erythrocytes is $D = 8.2 \pm 1.2 \times 10^{-9}$ cm^2/s at 25°C and $D = 2.1 \pm 0.4 \times 10^{-8}$ cm^2/s at 37°C, and varies ~50-fold between 1° and 42°C. The diffusion constants of lipid analogue rhodamine-B phosphatidylethanolamine (RBPE) are about twice those of DiI[5]. The temperature dependence and magnitude of D vary by up to a factor of 3 between species and are only influenced by donor age in prenatals. DiI[5] diffusibility is not perturbed by the presence of calcium or local anesthetics or by spectrin depletion (via mutation). However, lipid-analogue diffusibility in erythrocyte ghosts may differ from intact cells. Dietary hypercholesterolemia in rabbits reduces the diffusion coefficient and eliminates the characteristic break in Arrhenius plots of D found in all other cells studied except frog.

INTRODUCTION

The erythrocyte plasma membrane and its associated cytoskeleton is the most thoroughly understood and perhaps the most studied of all biomembranes (1). Because red cells are free of intracellular membranes, their plasma membrane components are readily analyzed; further, the availability of many membrane-related mutants has provided access to critical physiological parameters (2, 3). The unique spectrin-based cortical cytoskeleton appears responsible for the remarkable viscoelastic properties that enable the erythrocyte to squeeze undamaged through fine capillaries and permit the formation of durable hemoglobin-free membrane ghosts (4). Moreover, the lipid-class composition of erythrocyte membranes is stable: phospholipid, cholesterol, and neutral lipid ratios are genetically determined, although diet influences their hydrocarbon chain compositions (5). Lipid defects are associated with disorders such as muscular dystrophy (6) and hypercholesterolemia (7).

Mobility measurements of the membrane components in erythrocytes have uncovered many intriguing problems and apparent contradictions. Red cell ghost membrane microviscosity has been measured by observing the fluorescence depolarization associated with the rotation of small lipid-soluble molecules (7, 8) and indicates that the membrane lipids are highly fluid (for review of the method, see reference 9). Cherry has investigated the rotational diffusion of band 3 protein by monitoring the triplet-absorption spectral decay of attached chromophores (10–12) and finds that a temperature-dependent fraction of the band 3 protein experiences highly restricted rotation. Otherwise, the band 3 populations show no thermal influence in their rotation rates, implying that some mechanism other than temperature-dependent membrane viscosity is responsible for the observed inhibition. Fluorescence photobleaching measurements of the slow lateral diffusion of band 3 protein have been undertaken in ghosts by Peters et al. (13), Koppel et al. (14, 15), and Golan and Veatch (16). Fowler and Branton (17) find that at physiological temperatures, band 3 protein mixes gradually between ghost membranes fused with Sendai virus. Fowler and Bennett (18) have shown that a fraction of band 3 is attached through "ankyrin" to the spectrin-actin cytoskeleton, implying that the rotational and lateral diffusion of band 3 is regulated by cytoskeletal coupling in normal erythrocyte ghosts. Direct spectrin cross-linking also restricts band 3 mobility (19). Koppel et al. report that disruption of the ghost cytoskeleton by dephosphorylation or mutation releases some portion of band 3 for lateral diffusion with nearly the diffusion coefficient that is expected for viscous drag alone (15). Recent experiments on mammalian lymphocytes, fibroblasts, and muscle cells show that the formation of blebs (blisters) on cell membranes separates the membrane from most of the F-actin cytoskeleton and releases integral membrane proteins from natural constraints on diffusion so that their diffusion constants increase to about half the theoretical limit set by mem-

Reprint requests should be sent to Dr. Webb.

brane lipid viscosity (20, 21). Lipid diffusibility in bleb membranes increases only slightly, relative to the intact tissue membrane (20).

To date, structural interpolations from lysed to intact erythrocyte membranes have been routinely accepted, even though red blood cell lysis damages the spectrin network by irreversibly perturbing the intracellular calcium and ATP concentrations (22, 23) and by releasing spectrin into the supernatant (24). Concern with the potential effects of ghost-formation treatments led us to concentrate our diffusibility studies on intact erythrocytes in spite of the extra difficulties this entailed.

Measurements of lipid lateral diffusion by fluorescence photobleaching recovery (FPR) require incorporation of fluorescent lipid-analogue molecules into cell membranes, photobleaching some of this probe within a small area of an individual cell, and monitoring the subsequent recovery of fluorescence from the bleached spot as fresh fluorophore diffuses into it from the surrounding membrane (Fig. 1). Quantitative analysis of the time course of fluorescence recovery yields a characteristic recovery time, τ_D, which

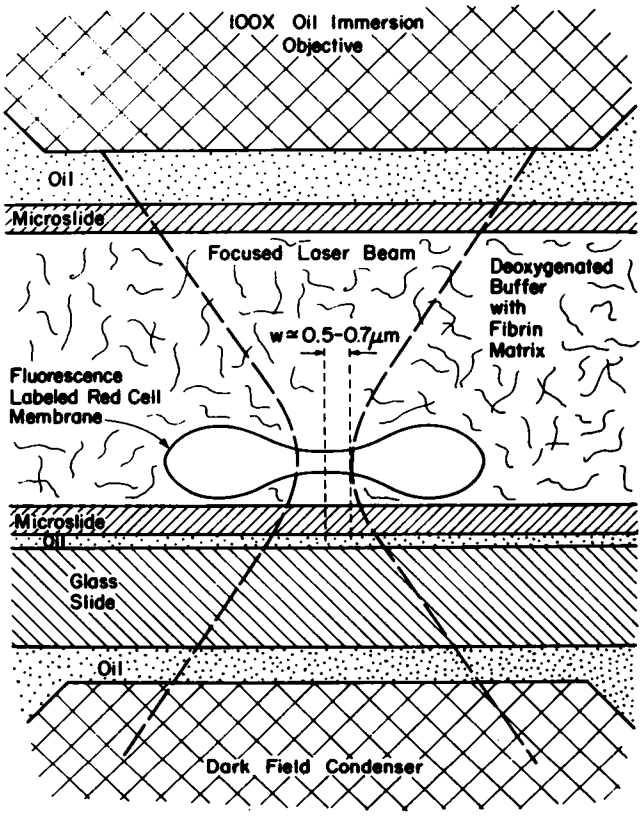

FIGURE 1 A cross-sectional view of a photobleaching experiment, showing the laser spot focused on the center of the cusp of an individual erythrocyte. Cells are immobilized by a fibrin matrix because more customary methods of treating glass surfaces with poly-l-lysine (73) or Lanthanum (74) induced visible morphological changes in the cell surface. Sample temperatures were set and regulated to within 0.2°C by thermally isolating and water jacketing the oil-immersion objective, condenser, and stage. Note that only the cell and beam are correctly scaled in this diagram.

may be related directly to the lipid analogue diffusibility coefficient D, and by the equations of Saffman and Delbrück, to membrane viscosity (25). FPR measurements done on tissue cells (12, 26–29), and, more recently, on normal- and high-cholesterol erythrocyte ghosts, have been reported (30, 31); however, two problems interfere with FPR experiments on intact erythrocytes: absorption of the excitation light by hemoglobin, and photolability of the erythrocytes in the presence of bleaching intensities on the order of 10,000 to 1,000,000 W/cm^2 (10, 32). These impediments were avoided by the use of infrared fluorophores excited in the deep red and by thorough sample deoxygenation. Although our detailed study of erythrocyte photosensitivity and stabilization techniques will be reported elsewhere, the present experiments were conducted under conditions where the intact erythrocytes were so stable to the incident laser power that exhaustive exposures (depleting of all of the probe in the entire cell membrane) to the ~1.5-μm diam, ~0.1-mW bleaching spot did not induce visible membrane photodamage. Such severe doses are at least 3,000 times those required for the usual series of FPR experiments on a cell.

MATERIALS AND METHODS

Labeling Protocol

40 μl of packed red cells were diluted in 8 ml of mouse blood plasma buffer (MB: 128 mM NaCl, 15 mM glucose, 10 mM HEPES [Research Organics, Inc., Cleveland, OH], 4.2 mM $NaHCO_3$, 3 mM KCl, 2 mM $MgCl_2$, 1 mM KH_2PO_4, pH 7.1, with 50 μg/ml gentamicin [Schering Corp., Kenilworth, NJ] added as a preservative) and centrifuged at 1,100 g for 3 min in Siliclad-treated (Clay Adams, Parisippany, NJ) disposable glass test tubes. The supernatant was removed by aspiration and the pellet was resuspended in MB. Following a second wash, 2 ml of this cell suspension was diluted to 8 ml with MB, and 80 μl of ethanol containing 0.01–0.02 mg/ml DiI[5] (Fig. 2 *A*) or 10–50 μM rhodamine-B phosphatidylethanolamine (RBPE) (Fig. 2 *B*) was added. The suspension was incubated with occasional agitation at room temperature for 15–30 min, after which the cells were washed 2–4 times. Following the final wash, the cell pellet was resuspended in 300 μl of MB, which contained 3–10 mg/ml of bovine fibrinogen (95% clottable; Miles Laboratories Inc., Elkhart, IN), if the sample was immobilized by clotting. For deoxygenation, ~90 μg of submitochondrial particle (SMP) protein/tube and a substrate of 20 mM succinate (Sigma Chemical Co., St. Louis, MO) were added. The SMP, prepared by the method of Beyer (34), were a gift of Edward Berry (Cornell University). To clot the sample, 10–50 units/ml of human thrombin (Sigma Chemical Co.) in MB was drawn into the first 1–4 mm of a 50-μm thick, 50-mm long pyrex microslide (Vitro Dynamics, Inc., Rockaway, NJ); capillary mixing occurred as the red cell suspension was then drawn in to fill the microslide.

All blood samples were labeled and ready for analysis within 3 h after drawing, with the exception of the human hypercholesterolemic (HCh) samples, which were prepared within 6–8 h after collection. Experiments lasted from 10–30 h; 3–5 independent blood samples were studied simultaneously. The order of temperature sequences was chosen to minimize the possible effects of sample deterioration, which was observed occasionally at temperatures over 30°C.

Probe Concentration

The lipid/probe ratio, a measure of the DiI[5] concentration in the cell membrane, was estimated by comparing the fluorescence of well-washed,

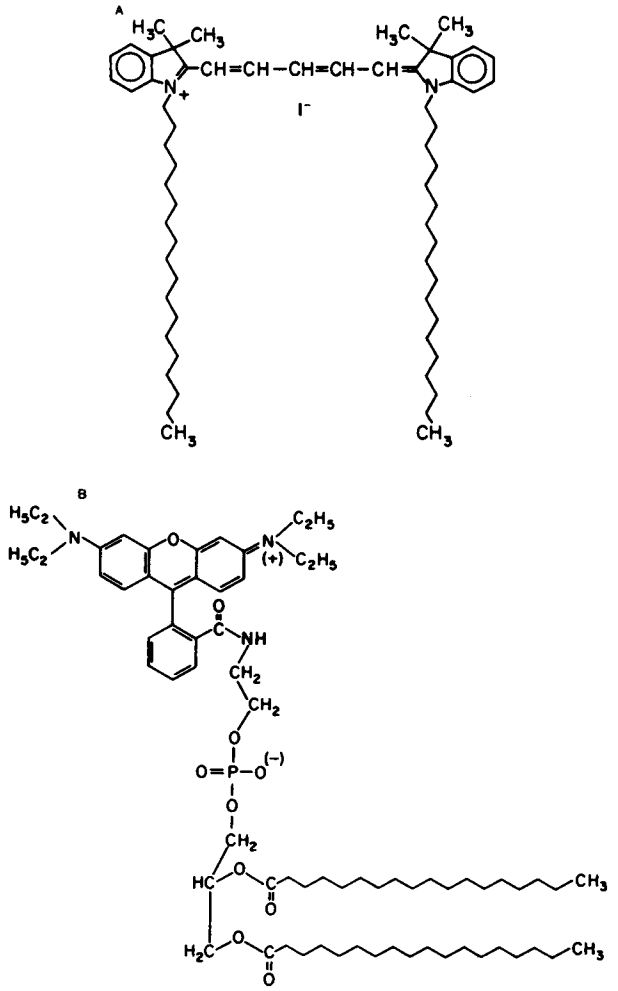

FIGURE 2 (*A*)3,3'-dioctadecylindodicarbocyanine iodide (DiI[5]) (gift of Alan Waggoner, Amherst College, MA), the principal fluorescent lipid analogue used in this work, was selected for its long-wavelength optical absorption spectrum and high fluorescence quantum efficiency (33). Optical absorptions due to intracellular hemoglobin and protoporphyrin were avoided by using 647 nm krypton-ion laser excitation (40). The peak absorption wavelength for DiI[5] in EtOH is 647 nm. (*B*)The phospholipidlike analogue rhodamine-B phosphatidylethanolamine (RBPE) (gift of Jeff Reidler, Cornell University) was used despite its mediocre incorporation properties as a control for the influence of lipid-analogue molecular structure on diffusibility results. RBPE required 568-nm laser excitation, which heightened the photosensitivity of intact erythrocytes (40). The peak absorption wavelength for DiI[5] in EtOH is 554 nm.

labeled erythrocyte suspensions that were lysed using 1% Triton X-100 (Sigma Chemical Co.) with unlabeled, Triton-lysed cell suspensions to which a known concentration of DiI[5] was added directly. The lipid concentration of these samples was calculated from their hematocrits as determined by hemoglobin absorption. All optical measurements were performed on a Jobin Yvon (Longjumeau, France) spectrofluorimeter integrated with a Princeton Applied Research (Princeton, NJ) model 1215 optical multichannel analyzer (OMA-2).

Red Blood Cell Collection

Adult mouse blood was drawn into a heparin-coated microhematocrit tube (Fisher Scientific Co., Rochester, NY) from a small incision made in a major tail artery. Young mice were exsanguinated by decapitation or heart puncture. Unless otherwise noted, the mice used in these experiments were of the random-bred Swiss albino strain (Blue Spruce Farms, Inc., Altamont, NY). Dystrophic (dy/dy) mice of the 129/REJ and C57BL/6J strains (Jackson Labs, Bar Harbor, ME) were either purchased or bred in our lab. Nondystrophic (+/?) littermates were used as controls in these experiments. The normoblastic (nb/nb), hemolytic (ha/ha), and spherocytotic (sph/sph) WBB6F$_1$ strain mouse mutants were the generous gift of Dr. Sheldon Bernstein (Jackson Labs). WBB6F$_1$ mutant erythrocytes required a 5–10 times higher DiI[5] concentration to obtain adequate fluorescence labeling and ~3 times higher fibrinogen and thrombin concentrations for satisfactory immobilization.

Human blood samples were obtained by Dr. Virginia Utermohlen (Cornell University) from assorted, apparently healthy volunteers by arm venipuncture and were collected in EDTA or heparin-coated vacutainer tubes (Fisher Scientific Co.). Hypercholesterolemic blood was obtained from a volunteer with diabetes-induced hyperlipidemia selected by Dr. Jerome Nosanchuk of the Tompkins County Hospital (Ithaca, NY). The serum cholesterol level of this donor, as assayed by the modified Liebermann-Burchard method with Hycel reagents (Houston, TX), was 530 mg/dl (control, 184 mg/dl) and the serum triglyceride level, as determined by enzymatic degradation with Hycel reagents was 6,100 mg/dl (control, 78 mg/dl). No membrane cholesterol comparison was made.

"Resealed" ghosts were prepared by following the procedure of Sheetz and Koppel (35). The final DiI[5]-labeled ghost suspension was refrigerated at ~4°C overnight for FPR experiments the next day. "Dilution-hemolysed" ghosts were made by the method of Thompson and Axelrod (30) and used promptly. A serum protein such as bovine serum albumin or fibrinogen was added to the buffer before mounting either ghost preparation, to reduce adhesion and rupture on the microslide surface (36). Both ghost suspensions were photobleached using our fibrin immobilization and SMP deoxygenation techniques.

New Zealand White female rabbit blood samples (gift of Barry Hughes, Cornell University) were obtained by standard ear incision techniques, using EDTA or heparin as the anticoagulant. HCh was induced by placing a rabbit on a 0.5 g cholesterol/d (0.5%) diet, and blood samples were taken from 9–28 wk after diet initiation. The blood serum cholesterol level was found by the method of Zak et al. (37) to be ~1,554 mg/dl (control, 140 mg/dl). Using the technique of Rose and Oklander (38), Barry Hughes found that the HCh rabbit had a membrane cholesterol level ~1.35 times normal, indicating that the membrane cholesterol mole percentage was elevated from the normal value of 47% (phospholipid/cholesterol ratio 0.89:1) to 55% (1.22:1).

Large adult Leopard frogs (West Jersey Biological Supply, Wennonah, NJ) were kept at room temperature and fed for 4–6 wk before blood samples were taken. Blood was obtained from major arteries in the lower leg, using ether and an ice bath as anesthetics. To stabilize frog erythrocytes against lysis within 4–6 h, we found it necessary to add 1 mM Ca^{+2} to the MB.

In studies of local anesthetics, fresh mouse red cells were labeled as outlined above and the final washed cell pellet was suspended in a Lidocaine or Procaine (Sigma Chemical Co.) doped MB solution. Diffusibility measurements were not started until the cells had been incubated in this solution for at least 1 h.

APPARATUS

For this research, the fluorescence photobleaching recovery (FPR) technology was extended beyond first generation instrumentation (28, 39) to increase accuracy and precision, to work with near-infrared fluorophores that minimize hemoglobin absorption, and to facilitate measurement of the very fast recovery recountered with lipid probe diffusion on small cells (40). A schematic diagram of the instrumentation is shown in Fig. 3. A krypton-ion laser beam is split into separate monitor and bleach beams by reflection from a mirrored optical flat (F1)(Virgo Optics, Stirling, NJ). Accurate bleaching pulses in the millisecond range are selected by staggering the opening and closing times of the two independent shutters

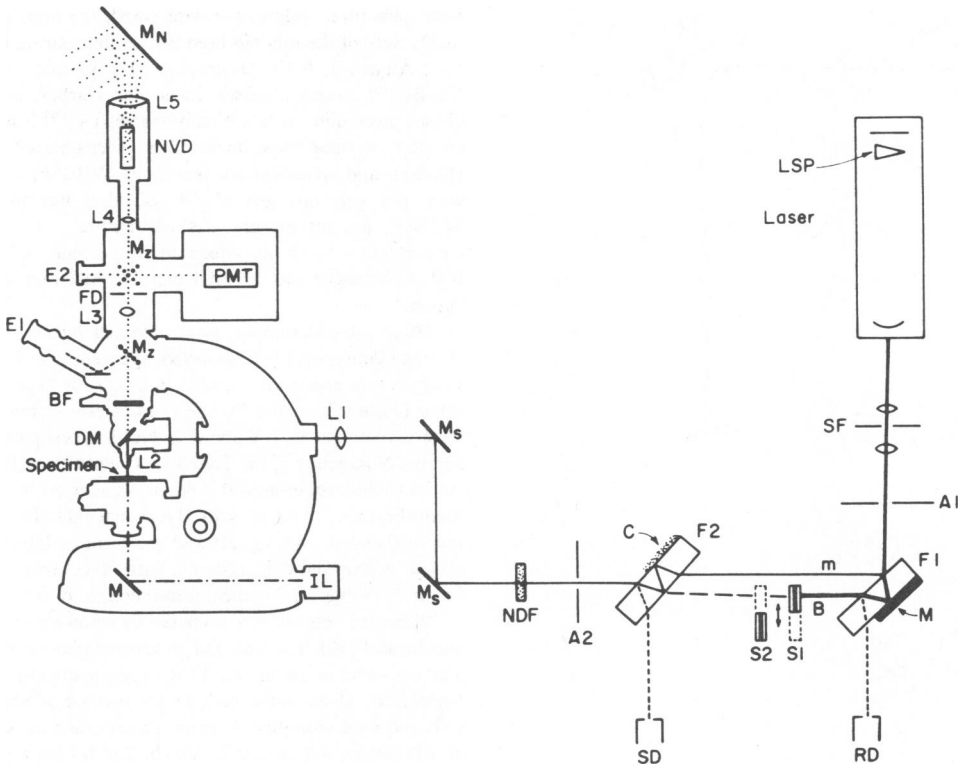

FIGURE 3 Overview of the photobleaching apparatus: *LSP*, tuning prism; *SF*, spatial filter; *A1*, *A2*, scatter-reducing apertures; *NDF*, stationary neutral density filters; *L1*, adjustable focusing lens; *DM*, dichroic mirror; *E1*, *E2*, eyepieces; *Mz*, movable mirrors. Other features and abbreviations are discussed in the text.

(S1, S2) that intercept the bleach beam. The monitor and bleach beams are then recombined by a matching optical flat (F2) to superimpose their optical paths to the specimen. Multiple reflections at the quartz-air interfaces of F1 and F2 largely determine the intensity ratio of the bleach and monitor beams (41). In our application, this ratio was fine tuned to ~3.6 OD by reducing the reflectivity of the second surface of F2 with a MgF_2 antireflection coating (C) (Evaporated Metal Films Corp., Ithaca, NY). An electronic switch disabled the photomultiplier tube (PMT) during bleaches to prevent anode damage, yet turned the tube back on within 1 ms after a bleach to measure the fluorescence recovery of the sample accurately. Photodiodes (RD, SD) compared the beam intensity both before and after the shutter to determine the exact length of each bleach pulse.

The cells were viewed with a Zeiss 100X, 0.8-NA oil-immersion dark-field objective lens (L2), yielding an image size that allowed the adjustable diaphragm (FD) for the PMT to be opened to ~1 mm. The barrier filter (BF) was constructed from three 40–50 nm band-pass, 6–8 cavity interference filters that were deposited on Suprasil substrates (Optical Thin Films, North Andover, MA). The microscope was also fitted with a night vision device (NVD) (Ni-Tec, Inc., Niles, IL) to enhance the visibility of the near-infrared (676 nm peak) DiI[5] fluorescence when focusing the beam on the sample.

An on-line PDP 11/20 computer (Digital Equipment Corp., Maynard, MA) allowed data acquisition rates of up to 0.5 ms per data point while controlling the apparatus and recording relevant experimental parameters. To accomodate fast sampling rates, the signal-to-noise ratio was enhanced by repeatedly bleaching the same spot on a single cell until 5–32 computer-synchronized recovery curves were accumulated. Because the lipid probe was always essentially 100% mobile, a simple averaging procedure was possible, provided that a recovery interval of at least 10 characteristic diffusion times (10 τ_D) was allowed between bleaches. No systematic trends in the data from repeated bleach sequences were found when analyzing the individual recovery curves of an averaged set, although overall probe depletion due to the finite area of the erythrocyte membrane could decrease the prebleach fluorescence intensity by ~10% during a bleaching sequence.

Computerized linear regression techniques that used an optimal convergence algorithm (42) generated three-parameter fits of the averaged time course of fluorescence recovery (Fig. 4) to the exact series solution of the diffusive recovery process (26). To test for and suppress possible measurement-noise artifacts at early recovery times ($t < 20\% \tau_D$) several fits were obtained for each recovery curve starting at various selected times after the bleach. The case that minimized the standard error of estimate was chosen for the best fit value of the characteristic diffusive recovery time, τ_D. Visual comparison of the theoretically calculated curves (Fig. 4) and the individual data points eliminated adventitious errors of the free parameters >15%. Further, a modified Student's *t*-test was used to estimate the statistical significance of marginal (~20%) differences in *D* between samples (43, 44). Variations were considered significant only when the Student's probability *P* was >0.95 (95%) over at least a 15°C temperature range.

Because the measured value of the diffusion constant *D* varies as the square of the radius of the focused laser spot on the surface of the cell, reliable radius measurements are essential to establish accurate, absolute values of *D*. Our convolution scan method, described by Schneider and Webb (45), directly determines beam radius from the "flow" recovery curve (26), which is generated by mechanically scanning a spot that has been bleached in a thin sample of immobilized fluorophore. Daily variations in beam radius were corrected by including a control sample of mouse erythrocytes in each run to standardize and normalize the results. This practice reduced the alignment-dependent uncertainty in *D* estimates from ~50% to a worst case of 20%.

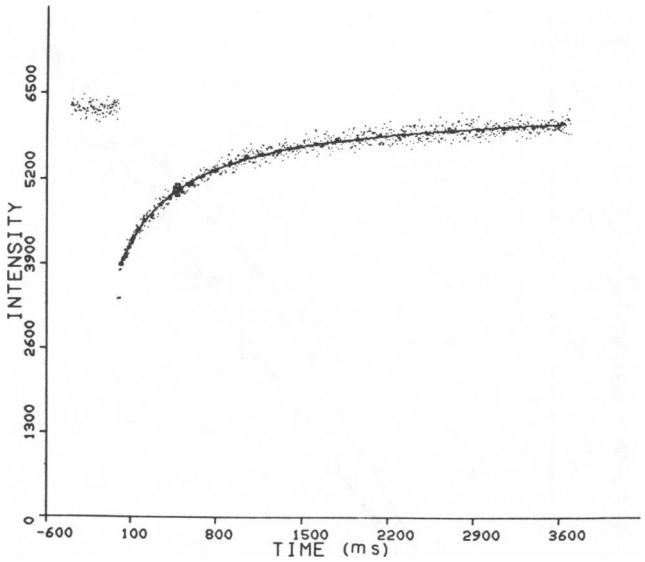

FIGURE 4 The results from a typical photobleaching experiment. 1,024 points were collected at 4 ms intervals for each of 19 photobleaches on the same spot of an individual cell. Data were averaged and computer fit to the theoretical recovery curve as described in the text. The small dots are the averaged data points from the 19 bleaches. The solid line (—) is the computer-generated best-fit recovery curve. The maltese cross marks the best-fit characteristic diffusive recovery time τ_D.

RESULTS

Our results are presented in the following order: First, diffusion-constant control values are established and the effects of deoxygenation, immobilization, cell shape, and beam position are summarized. Second, we present our results for normal erythrocytes from several species. Third, we consider the effects of several pathologies and treatments expected to produce membrane perturbations; these include hypercholesterolemia, donor age, cell lysis, spectrin depletion (anemia), muscular dystrophy, and treatment with local anesthetics.

Diffusibility Controls

We established a reproducible diffusion constant D for the lateral diffusibility of DiI[5] in the membranes of fresh, adult, albino mouse, intact erythrocytes of $D = 1.3 \pm 0.2 \times 10^{-8}$ cm^2/s at 25°C and $D = 3.1 \pm 0.4 \times 10^{-8}$ cm^2/s at 37°C. Typical lipid-to-probe ratios in these experiments were ~1,000:1, although ratios up to ~200:1 could be tolerated without perturbing D. RBPE in fresh, adult, normoblastic (nb/nb), intact erythrocytes gave a diffusion coefficient approximately two times faster ($D = 2.9 \pm 0.6 \times 10^{-8}$ cm^2/s at 25°C and $D = 6.8 \pm 1.2 \times 10^{-8}$ cm^2/s at 37°C), in general agreement with earlier RBPE and 3,3′-dioctadecylindocarbocyanine iodide (DiI[3]) mobility comparisons in model lipid bilayer membranes (46).

By using very weak bleaching intensities (<0.1 mW incident) at 647 nm, we measured DiI[5] diffusibility in intact erythrocytes without deoxygenation. Although visible membrane photodamage (puckering) normally occurred during repetitive bleaching, diffusibility results were only affected if the photobleached area of the membrane moved with respect to the focused beam.

With certain lots of microslides we found it possible to prepare red blood cell samples where a small population of cells spontaneously adhered to the pyrex surface. Statistical comparison of measurements made on the free (upper) membranes of such glass-immobilized controls with fibrin-immobilized preparations showed no significant differences in DiI[5] diffusibility. Further, measurements taken in the center of the cusp of biconcave discoids, on the crest surrounding the cusp of biconcave discoids, or in the center of either the upper or lower membrane of large (7–8 μm) diameter spheroids gave equivalent D values, implying that lipid diffusibility in the erythrocyte membrane is uniform throughout the cell surface. Consequently, once this uniformity between disks and large spheres was established, we routinely worked with spheroid cells, since the lesser curvature eased the alignment precision required to ensure that the beam was oriented normal to the membrane surface. Crenated cells were avoided, as surface profile convolutions within or near the photobleached spot would give misleading diffusion results (47).

No deviations were introduced in intact mouse red blood cell diffusibility by the addition of 1 mM calcium to the medium. No significant deviations in D were noted between frog intact cells (with calcium) and frog ghosts (without calcium), implying that calcium does not perturb frog red blood cell lipid diffusibility.

Submitochondrial Particles

The addition of phospholipid vesicles to an erythrocyte suspension introduces the danger that cholesterol, phospholipids, or even membrane proteins may interchange between the heterogeneous membranes (48). However, our controls demonstrate that SMP and red cells do not transfer membrane components in sufficient quantity to modify lipid fluidity: (*a*) Omission of SMP from the media introduced no significant change in probe diffusibility at very low bleaching doses; (*b*) incubation of labeled erythrocytes with SMP at 37°C did not induce appreciable hemolysis within the time scale of FPR experiments (30 h maximum), whereas incubation with dimyristoylphosphatidylcholine (DMPC) vesicles completely lyses red blood cells within 1 h under similar conditions (48). Such stability is surprising in view of our observation that RBPE rapidly transfers from normal cells to SMP (a similar effect is reported by Johnson et al. [49]). However, Wray H. Huestis (Stanford University, personal communication) notes that vesicles containing over 2% phosphatidylserine (PS) do not interchange membrane components with red blood cells and suggests that a net negative charge

inhibits cell-vesicle transfer. The large fraction of cardiolipin in mitochondrial inner membranes may be responsible for a parallel effect in our system.

Factors Influencing Diffusibility

Species. Differences in the human, mouse, and frog diffusibility data shown in Fig. 5 are statistically significant at each individual temperature with a probability $P > 99.9\%$ in nearly all cases (at 25°C, $D_{human} = 8.4 \pm 1.1 \times 10^{-9}$, $D_{mouse} = 13. \pm 2. \times 10^{-9}$, $D_{frog} = 5.3 \pm 0.6 \times 10^{-9}$ cm^2/s). The clear break in the linearity of D in the mouse and human plots near 12°C represents a shift in the apparent activation energy (E_a) from ~14 to ~25 kcal/mol. This feature is absent in the frog curve, which shows a uniform E_a of ~17 kcal/mol. Diffusibility in normal rabbit red blood cells (Fig. 6) parallels that of human and mouse

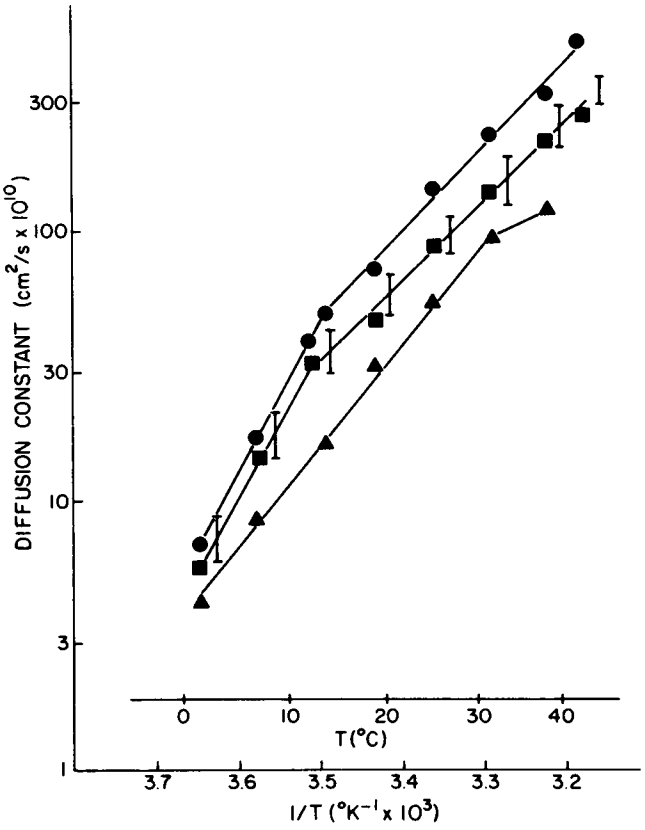

FIGURE 5 Diffusion results for DiI[5]-labeled normal adult mouse (●), human (■), and frog (▲) intact erythrocytes. These Arrhenius plots represent composites for eight mouse, five human, and two frog cell preparations, each from a different donor and each run on a different day with an average of 24, 19, and 14 cells measured per respective data point. The break in the frog curve over 32°C may be an artifact of cell degradation as a precursor to thermally induced lysis which occurs near 40°C; such deviations were also observed in degrading mouse and human samples. The error bars in these plots have been slightly shifted for clarity and represent the average standard deviation of all isothermal data points clustered to the left of each bar.

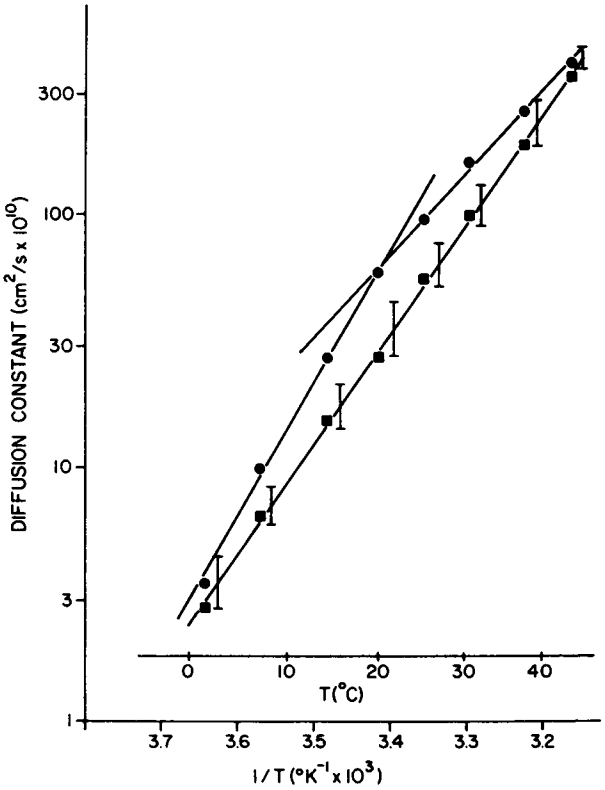

FIGURE 6 Diffusion results for DiI[5]-labeled normal (●) and dietary-induced hypercholesterolemic (HCh) rabbit intact erythrocytes (■). The statistical significance of the differences in these curves exceeds $P > 99.9\%$, except at the temperature extremes, where the certainty $P > 97.5\%$. The minimum correlation coefficient of the linear fits shown exceeds 0.9985. For further discussion, see text.

cells, but the apparent slope change occurs at a somewhat higher temperature (near 20°C).

Hypercholesterolemia. In Fig. 6, the DiI[5] diffusion coefficients from dietary-induced HCh rabbit erythrocytes are contrasted with data from normal rabbit erythrocytes. Note that the elevated membrane cholesterol level depresses membrane diffusibility significantly and abolishes the apparent slope change. Our worst available case of human HCh (data not shown) showed a ~34% reduction in diffusibility below 20°C but nothing significant over 25°C. Further, this effect was not sufficient to abolish the apparent slope break seen in normal cells near 12°C.

Donor Age. A comparison of DiI[5] diffusibility on intact erythrocytes from prenatal (18–20 d gestation), neonatal (<18 h old), and adult (>12 wk old) mice shows that prenatal erythrocytes have slightly reduced diffusion coefficients over most of their temperature range (average reduction ~30% with $P > 95.0\%$, data not shown). Neonatal and juvenile (2 wk old) cells show little significant deviation from adult controls (data not shown).

Lysis. Table I summarizes the diffusion results obtained from our preparations of resealed and dilution-hemolysed human ghosts. Resealed ghosts show no significant deviations from intact cells over ~20°C; however, at lower temperatures resealed ghost diffusibility is ~30% slower than intact cells with $P > 99.0\%$. Dilution-hemolysed ghosts show approximately twofold slower diffusibility throughout the entire temperature range, a deviation that is significant with a minimum $P > 99.5\%$.

Factors That Do Not Influence Diffusibility

Mutation. No significant differences in lipid diffusibility are apparent in the dystrophic or anemic mutants at temperatures over ~20°C (data not shown). The data at low temperatures exhibit more scatter, but have no obvious correlation with the degree of spectrin depletion. However, WBB6F$_1$ mutant cells do show deviant behavior in other areas: they readily absorb RBPE but not DiI[5], a response exactly opposite that of normal erythrocytes. Furthermore, they would not adhere to pyrex nor were they easily immobilized in fibrin clots. Such behavior may be due to an altered electrostatic charge on the membrane exterior induced by an abnormal lipid, protein, or polysaccharide composition.

Anesthetics. Although 7.2 mM concentrations of Lidocaine reduced and 9.4 mM concentrations of Procaine increased the diffusibility of DiI[5] (data not shown), neither of these trends proved to be statistically significant when analyzed by the modified Student's *t*-test.

DISCUSSION

We have measured the lateral diffusion of the fluorescent lipid analogues DiI[5] and RBPE in individual, intact erythrocyte membranes under normal and abnormal conditions and observe that these probes are highly mobile at all temperatures studied. This result shows that these lipid analogues, and presumably the erythrocyte membrane lipids themselves, are free to diffuse in the plane of the membrane, in striking contrast to band 3 membrane protein, which is comparatively immobile ($D \simeq 10^{-11}$ cm^2/s at 25°C) on normal erythrocytes (14–16, 50; and our unpublished results). Therefore, the "land-locked lake" membrane model, where dense networks of integral membrane protein form isolated pockets of membrane components and restrict lateral diffusion over large areas, does not appear to be a viable hypothesis for the erythrocyte membrane lipids, although band 3 diffusion may be constrained in this manner. However, any strong association of mobile probe molecules with relatively immobile proteins could retard diffusion, reducing the effective diffusion constant (51–53). If the binding mechanism itself was temperature dependent, its influence would be reflected in the observed diffusibility. Our results do not exclude such evanescent binding beyond setting the upper limit for probe-protein bound residence time to be appreciably shorter than the measured recovery time τ_D.

TABLE I
DiI[5] DIFFUSIBILITY IN HUMAN ERYTHROCYTES AND GHOSTS*

Sample	Diffusion constant ($D \times 10^9$ cm^2/s) at			
	1.5°C	12.1°C	25.1°C	36.9°C
Intact cells	0.68 ± 0.15	3.1 ± 0.48	8.2 ± 1.2	21. ± 4.6
Resealed ghosts‡	0.50 ± 0.20	2.2 ± 0.76	7.8 ± 2.3	19. ± 4.4
Dilution ghosts§	0.36 ± 0.09	1.6 ± 0.26	6.3 ± 2.1	15. ± 3.1

*A D value represents the average of 12–19 individual cells per sample measured at each temperature on our apparatus. The standard deviation for each average D is given.
‡Ghosts prepared following reference 35.
§Ghosts prepared following reference 30.

Comparison with Ghost Microviscosity

Cooper et al. (8) assayed human ghost membrane microviscosity over the temperature range of 10° to 40°C and observed that the apparent activation energy (E_a) of membrane viscosity decreased as the cholesterol mole percent increased. (Values ranged from 11.8 kcal/mol in depleted membranes to 8.3 in normals and 5.8 in HCh membranes.) In contrast, E_a, deduced from the lateral diffusion data in Fig. 6, shows a value of 20. kcal/mol for rabbit HCh, and a more complex response in normals (25. kcal/mol below 20°C, 15. above 20°C). Comparison of microviscosity and lateral diffusion results on normal erythrocytes reveals not only a twofold discrepancy in the relative magnitudes of E_a, but also a qualitative difference in that microviscosity data never show the slope break that is characteristic of FPR data. Because it is quite probable that the E_a are determined by the temperature dependence of molecular order associated with membrane phase transitions rather than an actual thermally excited rate process, this disparity may reflect the fact that microviscosity measurements are primarily sensitive to hydrocarbon chain disorder (9), while FPR-probe diffusibility is regulated by both chain disorder and molecular packing within the bilayer. Thus lateral diffusibility provides a different measure of lipid properties that involves interactions over the full thickness of the membrane.

Comparison with Band 3 Rotational and Lateral Diffusion

Cherry's investigations (reviewed in reference 12) of the rotational mobility of band 3 protein show the existence of two populations of mobile protein whose respective rotational relaxation times are not temperature dependent. In

view of the large temperature dependence observed in our lipid analogue diffusibility studies, it appears that lipid viscosity does not limit the rotational mobility of either population. Even at 37°C, membrane viscosity estimates (25) derived from these lateral and rotational results differ by a factor of 2.

In their FPR experiments on ghost membranes, Golan and Veatch (16) found ionic conditions that pushed band 3 lateral diffusion to $D = 2 \times 10^{-9}$ cm^2/s at 37°C. However, even this value is fourfold slower than what our lipid results would predict (25). Under more normal conditions lipid diffusibility in erythrocytes is 50- to 100-fold too fast for lipid viscosity to be the limiting factor in band 3 lateral diffusion. This implies that protein-protein interactions are responsible for low band 3 diffusibility.

Comparison with Artificial Model Membranes

Artificial multibilayer systems have been extensively studied as simple models of membrane properties and phase transitions. In pure DMPC or dipalmitoylphosphatidylcholine (DPPC) multibilayers, cholesterol is known to abolish sharp phase transitions in D (54–56). However, any sophisticated comparison of binary mixture models with erythrocyte membranes is nontrivial, as red cells are known to possess marked phospholipid and chain-length inhomogeneity (5) and a distinct, asymmetric distribution of lipids between the inner and outer membrane surfaces (1). Nevertheless, these models closely approximate the diffusibility properties of intact erythrocytes at temperatures over 12°C. D values of $\sim 1.3 \times 10^{-8}$ cm^2/s at 25°C and E_a of 9–18 kcal/mol have been reported for NBD-PE [phosphatidyl-*N*-(4-nitrobenzo-2-oxa-1,3-diazole)ethanolamine] in DMPC-cholesterol (1:1) model systems (55, 56).

Our results on normal mammalian erythrocytes (Figs. 5 and 6) show a distinct two-region response in the temperature dependence of diffusibility, paralleling the observations of many previous and diverse erythrocyte fluidity studies (^{31}P NMR [57], raman spectroscopy of native caratenoids [58, 59], viscosity variations in suspensions of sonicated membrane vesicles [60], and electron spin-label resonance [61]). It is particularly significant that HCh rabbit erythrocytes (Fig. 6), whose cholesterol level is 55 mol % instead of the normal 47 mol %, lack this break point. Lentz et al. (62) have characterized the phase regions of DPPC-cholesterol mixtures and proposed the existence of a two-phase region at high (40–50 mol %) cholesterol levels that undergoes a transition to a single-phase region at high temperatures or higher cholesterol levels (>50 mol %). As slope breaks in D are commonly interpreted as phase transitions in model systems, the transition we observe in normal mammalian red blood cells near 12° to 20°C may signal the presence of a phase boundary similar to that seen in model systems (62). Note that the frog, a polykilothermic (cold-blooded) amphibian, exhibits a uniform temperature dependence over the entire range studied, implying that frog red blood cells have a lipid/cholesterol ratio that maintains the membrane in a single-phase region over broad temperature variations. Unfortunately, no data are available on the lipid composition of frog erythrocytes to corroborate this hypothesis from model systems.

Comparison between Intact Cells and Ghosts

Numerous investigators have reported that the membrane properties of intact cells differ significantly from ghosts. Tanaka and Ohnishi (61) found deviations in microviscosity that were attributed to a breakdown of the membrane lipid asymmetry during or following lysis. Such a perturbation may be responsible for the changes in lateral diffusibility that we observe in ghosts (Table I): those prepared by a gentle Tris-resealing method (35) differ slightly from intact cells, while a more severe preparation technique (30), in which we observed membrane blebbing, yields ghosts with quite significant deviations.

Two- to fourfold deviations in D are apparent between our DiI[5] ghost studies and those using DiI[3] (30, 31). Comparison of experimental conditions (Table II) suggests that these discrepancies may be at least partially attributable to excessively high label concentrations and/or the high bleaching energies required by DiI[3], which is ~250 times more photostable than DiI[5] (40). Kapitza and Sackmann (31), measuring ghosts lysed in whole plasma by a 5% ethanol labeling technique, used apparent bleaching times ~125 times longer and DiI[3] labeling concentrations ~10-fold higher than in our present experiments. Under these conditions, membrane photodamage and heating (63) may occur, although it is more likely that the unusually long bleach time, violating $t_{bleach} \ll \tau_D$, perturbs the measurement. Thompson and Axelrod (30) noted that multiple bleaches of a single spot affected their recovery rates on dilution-hemolysed ghosts, suggesting photodamage had occurred.

Negative Effectors of Diffusibility

Spectrin. It is well established that certain mice anemias stem from a spectrin deficiency or dysfunction (3). Recently Koppel et al. (14, 15) have shown that band 3 is ~50 times more mobile in spherocytotic (sph/sph) ghosts than in normals. As we detect no significant differences in DiI[5] diffusibility between mutant and normal intact red blood cells, we infer that the erythrocyte integral membrane proteins that are normally coupled to the spectrin network exert no detectable influence on lipid diffusibility under physiological conditions.

Cell Age. Because their circulation lifetime is <1 d, red blood cell membranes from sph/sph, ha/ha, and

TABLE II
COMPARISON OF PUBLISHED PHOTOBLEACHING CONDITIONS AND RESULTS ON HUMAN ERYTHROCYTES

Group	Bleach beam characteristics					Protection	Probe	Probe concentration
	λ	Area	Power*	Duration	Total dose			
	nm	*μm²*			*μJ/μm²*			*μg/ml cells*
Thompson	514	0.66	2–4 mW	3–6 ms	18.2	none	DiI[3]	3–17
Kapitza	488	7.0	~10 μW‡	0.25–1 s	~0.4‡	none	DiI[3]	~100
Bloom	647	1.80	0.1 mW	3–4 ms	0.17	deoxygenation	DiI[5]	10–20

Group	Sample	*D* at 25°C	E_a
		cm²/s × *10⁹*	*kcal/mol*
Thompson§	dilution ghosts	1.8	3.7
Kapitza‖	5% ethanol ghosts	~3	12.0
Bloom	intact cells	8.2	13.2
	dilution ghosts	6.3	~13
	resealed ghosts	7.8	~13

*Incident beam power measured at objective.
‡Estimates of beam power and dose were obtained by personal communication with H. G. Kapitza.
§See reference 30.
‖See reference 31.

nb/nb mutants have a lipid and cholesterol content similar to that of the young red blood cells in normal mice (64). Therefore, diffusibility studies of mutant and normal adult erythrocytes not only test the influence of spectrin content on lipid diffusibility, but they also compare young and old (normal) cell populations. While the deviations observed in diffusibility below 20°C may be due to these age-related compositional differences, the fact that no significant perturbation in lipid diffusibility is observed at physiological temperatures implies that neither spectrin content nor cell age significantly affect probe diffusibility, unless both perturbations complement one another.

Muscular Dystrophy. Some forms of muscular dystrophy are known to induce morphological and fluidity changes in erythrocyte membranes, implying that these forms of the disease may be induced by a systemic (general) membrane defect (6, 65). Our studies on intact erythrocytes from readily available mouse mutants show that both the 129/ReJ and C57BL/6J strains have no detectable deviation from normal controls in their lateral diffusibility over the temperature range from 1° to 40°C. This result, in agreement with the microviscosity studies of Rubasamen et al. (66) on 129/ReJ ghosts, strengthens the view that the dystrophy of these mouse strains is not the result of a genetic, systemic membrane disorder.

Local Anesthetics. The exact locus of anesthetic action remains unclear, with a vast amount of data accumulated that suggests a mechanism involving lipid fluidization (67, 68); other research implicates calcium-ion partitioning or intracellular-ATP depletion mechanisms (69, 70). However, we found no statistically significant modulation of DiI[5] diffusibility on intact erythrocytes that were treated with the anesthetics Lidocaine or Procaine at concentrations approximately equal to or greater than those used by Tsong et al. (68) and Gazitt et al. (69). This result weakens the hypothesis that anesthetics function by perturbing lipid mobility.

Donor age. Kehry et al. (71) compared the lipid mobility of neonatal and adult human erythrocytes but found no distinguishable microviscosity differences. However, Kapitulnik et al. (72) observed that the fluidity of rat liver microsomal membranes increases at birth. Our results appear to confirm both of the above tendencies: DiI[5] diffusibility differences between neonatal, juvenile, and adult erythrocytes are insignificant, but prenatal red blood cells appear to deviate slightly, but significantly, from older donor cells.

CONCLUSIONS

The intact erythrocyte membrane has a fluid lipid phase in which lateral diffusibility exhibits a strong temperature dependence, approximating that seen above ~12°C in tissue cells such as myotubes (28) and in binary lipid/cholesterol model systems (56). The 100% mobility of probes and their independence of factors that sharply perturb band 3 diffusibility imply that interaction with membrane proteins does not substantially restrict the free diffusion of lipids over the erythrocyte surface. Conversely, lipid viscosity does not seem to limit the lateral or rotational mobility of band 3. Small differences in *D* are detectable between species but not among normal donors of a single species, suggesting that erythrocyte membrane lipid diffusibility is genetically determined. The distinct slope change seen in the *D* of normal mammalian red cells near 12° to 20°C is not caused by lipid-protein interaction, as it occurs in spectrin-depleted mutants and in cells treated with Lidocaine or calcium, which aggregate intramembrane proteins. This break in slope may signal a transition from a single to a mixed-phase membrane composition at lower temperatures. Higher than normal cholesterol levels reduce lipid diffusibility and eliminate

this transition. Comparison of these results with simple model systems (62) suggests that the red blood cell membrane is in a single-phase state under normal physiological conditions.

Significant differences in lipid diffusibility between resealed or dilution-hemolysed ghosts and intact erythrocytes are particularly apparent at low temperatures, suggesting that some membrane or lipid alterations accompany lysis and perturb the ultrastructure of the membrane. However, the negative results obtained with physiologically effective doses of local anesthetics imply that fluidity perturbation is not the principal mechanism of drug action. Further, our studies suggest that the 129/ReJ and C57BL/6J mouse muscular dystrophies are not attributable to a systemic membrane lipid-diffusibility deficiency.

The authors wish to thank Larry Barak and Peter Hinkle for their advice and suggestions during many critical phases of this research; Sheldon Bernstein, Jerome Nosanchuk, and Barry Hughes for their provision and analysis of important blood samples; and Marilyn Schneider, Rick Cochran, and Nancy Signorelli for their technical contributions and assistance.

This work was supported by National Institutes of Health grants GM21661B, CA14454, National Science Foundation grant 77-003111, and use of the facilities of the Materials Science Center at Cornell. Dr. Bloom was a predoctoral trainee under National Institutes of Health grant GM07273.

Received for publication 10 August 1982 and in final form 17 January 1983.

REFERENCES

1. Marchesi, V. T., H. Furthmayr, and M. Tomita. 1976. The red cell membrane. *Annu. Rev. Biochem.* 45:667–698.
2. Schekman, R., and S. J. Singer. 1976. Clustering and endocytosis of membrane receptors can be induced in mature erythrocytes of neonatal but not adult humans. *Proc. Natl. Acad. Sci. USA.* 73:4075–4079.
3. Lux, S. E., B. Pease, M. B. Tomaselli, K. M. John, and S. E. Bernstein. 1979. Hemolytic anemias associated with deficient or dysfunctional spectrin. *In* Normal and Abnormal Red Cell Membranes. S. Lux, V. Marchesi, and C. Fox, editors. Alan R. Liss, Inc., New York. 463–469.
4. Evans, E. A., and R. M. Hochmuth. 1977. A solid-liquid composite model of the red cell membrane. *J. Membrane Biol.* 30:351–362.
5. Nelson, G. J. 1972. Lipid composition and metabolism of erythrocytes. *In* Blood Lipids and Lipoproteins: Quantitation, Composition, and Metabolism. G. J. Nelson, editor. Wiley-Interscience, New York. 317–386.
6. Butterfield, D. A. 1977. Electron spin resonance studies of erythrocyte membranes in muscular dystrophy. *Accounts. Chem. Res.* 10:111–116.
7. Cooper, R. A., J. R. Durocher, and M. H. Leslie. 1977. Decreased fluidity of red cell membrane lipids in abetalipoproteinemia. *J. Clin. Invest.* 60:115–121.
8. Cooper, R. A., M. H. Leslie, S. Fischkoff, M. Shinitzky, and S. J. Shattil. 1978. Factors influencing the lipid composition and fluidity of red cell membranes in vitro: production of red cells possessing more than two cholesterols per phospholipid. *Biochemistry.* 17:327–331.
9. Shinitzky, M., and Y. Barenholz. 1978. Fluidity parameters of lipid regions determined by fluorescence polarization. *Biochim. Biophys. Acta.* 515:367–394.
10. Nigg, E. A., M. Kessler, and R. J. Cherry. 1979. Labeling of human erythrocyte membranes with eosin probes used for protein diffusion measurements: inhibition of anion transport and photooxidative inactivation of acetylcholinesterase. *Biochim. Biophys. Acta.* 550:328–340.
11. Nigg, E. A., and R. J. Cherry. 1979. Influence of temperature and cholesterol on the rotational diffusion of band 3 in the human erythrocyte membrane. *Biochemistry.* 18:3457–3465.
12. Cherry, R. J. 1979. Rotational and lateral diffusion of membrane proteins. *Biochim. Biophys. Acta.* 559:289–327.
13. Peters, R., J. Peters, K. H. Tews, and W. Bahr. 1974. A microfluorimetric study of translational diffusion in erythrocyte membranes. *Biochim. Biophys. Acta.* 367:282–294.
14. Koppel, D. E., M. P. Sheetz, and M. Schindler. 1980. Lateral diffusion in biological membranes: a normal-mode analysis of diffusion on a spherical surface. *Biophys. J.* 30:187–192.
15. Koppel, D. E., M. P. Sheetz, and M. Schindler. 1981. Matrix control of protein diffusion in biological membranes. *Proc. Natl. Acad. Sci. USA.* 78:3576–3580.
16. Golan, D. E., and W. Veatch. 1980. Lateral mobility of band 3 in the human erythrocyte membrane studied by fluorescence photobleaching recovery: evidence for control by cytoskeletal interactions. *Proc. Natl. Acad. Sci. USA.* 77:2537–2541.
17. Fowler, V., and D. Branton. 1977. Lateral mobility of human erythrocyte integral membrane proteins. *Nature (Lond.).* 268:23–26.
18. Fowler, V., and V. Bennett. 1978. Association of spectrin with its membrane attachment site restricts lateral mobility of human erythrocyte integral membrane proteins. *J. Supramol. Struct.* 8:215–221.
19. Smith, D. K., and J. Palek. 1982. Modulation of lateral mobility of band 3 in the red cell membrane by oxidative cross-linking of spectrin. *Nature (Lond.)* 297:424–425.
20. Webb, W. W., L. S. Barak, D. W. Tank, and E.-S. Wu. 1981. Molecular mobility on the cell surface. *Biochem. Soc. Symp.* 46:191–205.
21. Tank, D. W., E.-S. Wu, and W. W. Webb. 1982. Enhanced molecular diffusibility in muscle membrane blebs: release of lateral constraints. *J. Cell Biol.* 92:207–212.
22. Kirkpatrick, F. H. 1976. Spectrin: current understanding of its physical, biochemical, and functional properties. *Life Sci.* 19:1–18.
23. Lorand, L., G. E. Siefring, and L. Lowe-Krentz. 1978. Formation of α-glutamyl-ϵ-lysine bridges between membrane proteins by a Ca^{++}-regulated enzyme in intact erythrocytes. *J. Supramol. Struct.* 9:427–440.
24. Kansu, E., S. H. Krasnow, and S. K. Ballas. 1980. Spectrin loss during in vitro red cell lysis. *Biochim. Biophys. Acta.* 596:18–27.
25. Saffman, P. G., and M. Delbruck. 1975. Brownian motion in biological membranes. *Proc. Natl. Acad. Sci. USA.* 72:3111–3113.
26. Axelrod, D., D. E. Koppel, J. Schlessinger, E. E. Elson, and W. W. Webb. 1976. Mobility measurements by analysis of fluorescence photobleaching recovery kinetics. *Biophys. J.* 16:1055–1069.
27. Schlessinger, J., D. E. Koppel, D. Axelrod, K. Jacobson, W. W. Webb, and E. L. Elson. 1976. Lateral transport on cell membranes: mobility of concanavalin A receptors on myoblasts. *Proc. Natl. Acad. Sci. USA.* 73:2409–2413.
28. Axelrod, D., A. Wight, W. Webb, and A. Horwitz. 1978. Influence of membrane lipids on acetylcholine receptor and lipid probe diffusion in cultured myotube membrane. *Biochemistry.* 17:3604–3609.
29. Jacobson, K., Y. Hou, and J. Wojcieszyn. 1978. Evidence for lack of damage during photobleaching measurements of the lateral mobility of cell surface components. *Exp. Cell Res.* 116:179–189.
30. Thompson, N. L., and D. Axelrod. 1980. Reduced lateral mobility of

fluorescent lipid probe in cholesterol-depleted erythrocyte membranes. *Biochim. Biophys. Acta.* 597:155–165.
31. Kapitza, H. G., and E. Sackmann. 1980. Local measurement of lateral motion in erythrocyte membranes by photobleaching technique. *Biochim. Biophys. Acta.* 595:56–64.
32. Schothorst, A., J. Van Steveninck, L. N. Went, and D. Suurmond. 1970. Protoporphyrin induced photohemolysis in protoporphyria and in normal cells. *Clin. Chim. Acta.* 28:41–49.
33. Sims, P. J., A. S. Waggoner, C.-H. Wang, and J. F. Hoffman. 1974. Studies on the mechanism by which cyanine dyes measure membrane potential in red blood cells and phosphatidylcholine vesicles. *Biochemistry.* 13:3315–3330.
34. Beyer, R. E. 1967. Preparation, properties, and conditions for assay of phosphorylating electron transport particles (ETPH) and its variations. *Methods Enzymol.* 10:186–194.
35. Sheetz, M. P., and D. E. Koppel. 1979. Membrane damage caused by irradiation of fluorescent concanavalin A. *Proc. Natl. Acad. Sci. USA.* 76:3314–3317.
36. Brecher, G., and M. Bessis. 1972. Present status of spiculed red cells and their relationship to the discocyte-echinocyte transformation: a critical review. *Blood.* 40:333–343.
37. Zak, B., N. Moss, A. J. Boyle, and A. Zlatkis. 1954. Reactions of certain unsaturated steroids with acid iron reagent. *Anal. Chem.* 26:776–777.
38. Rose, H. G., and M. Oklander. 1965. Improved procedure for the extraction of lipids from human erythrocytes. *J. Lipid Res.* 6:428–431.
39. Koppel, D. E., D. Axelrod, J. Schlessinger, E. L. Elson, and W. W. Webb. 1976. Dynamics of fluorescence marker concentration as a probe of mobility. *Biophys. J.* 16:1315–1329.
40. Bloom, J. A. 1980. The lateral mobility of fluorescent lipid analogs in the membranes of intact erythrocytes. Ph.D. dissertation, Cornell University, Ithaca, N.Y.
41. Koppel, D. E. 1979. Fluorescence redistribution after photobleaching: a new multipoint analysis of membrane translational dynamics. *Biophys. J.* 28:281–292.
42. Powell, M. J. D. 1964. An efficient method for finding the minimum of a function of several variables without calculating derivatives. *The Computer Journal.* 7:155–162.
43. Meada, T., C. Eldridge, S. Toyama, S. Ohnishi, E. L. Elson, and W. W. Webb. 1979. Membrane receptor mobility changes by Sendai virus. *Exp. Cell Res.* 123:333–343.
44. Brownlee, K. A. 1965. Statistical Theory and Methodology in Science and Engineering. John Wiley & Sons, Inc., New York. 299.
45. Schneider, M. B., and W. W. Webb. 1981. Measurement of submicron laser beam radii. *Appl. Opt.* 20:1382–1388.
46. Fahey, P. F., D. E. Koppel, L. S. Barak, D. E. Wolf, E. L. Elson, and W. W. Webb. 1977. Lateral diffusion in planar lipid bilayers. *Science (Wash. DC).* 195:305–306.
47. Aizenbud, B., and N. D. Gershon. 1980. Diffusion of molecules on biological membranes of nonplanar form. *Fed. Proc.* 39:1980.
48. Huestis, W. H. 1977. A sodium-specific membrane permeability defect induced by phospholipid vesicle treatment of erythrocytes. *J. Biol. Chem.* 252:6764–6768.
49. Johnson, L. V., M. L. Walsh, and L. B. Chen. 1980. Localization of mitochondria in living cells with rhodamine 123. *Proc. Natl. Acad. Sci. USA.* 77:990–994.
50. Schindler, M., D. E. Koppel, and M. P. Sheetz. 1980. Modulation of membrane protein lateral mobility by polyphosphates and polyamines. *Proc. Natl. Acad. Sci. USA.* 77:1457–1461.
51. Magde, D., E. L. Elson, and W. W. Webb. 1972. Thermodynamic fluctuations in a reacting system: measurement by fluorescence correlation spectroscopy. *Phys. Rev. Lett.* 29:705–708.
52. Elson, E. L., and D. Magde. 1974. Fluorescence correlation spectroscopy. I. Conceptual basis and theory. *Biopolymers.* 13:1–27.
53. Magde, D., E. L. Elson, and W. W. Webb. 1974. Fluorescence correlation spectroscopy. II. An experimental realization. *Biopolymers.* 13:29–61.
54. Fahey, P. F., and W. W. Webb. 1978. Lateral diffusion in phospholipid bilayer membranes and multilamellar liquid crystals. *Biochemistry.* 17:3046–3053.
55. Wu, E.-S., K. Jacobson, and D. Papahadjopoulos. 1977. Lateral diffusion in phospholipid multibilayers measured by fluorescence recovery after photobleaching. *Biochemistry.* 16:3936–3941.
56. Rubenstein, J. L. R., B. A. Smith, and H. M. McConnell. 1979. Lateral diffusion in binary mixtures of cholesterol and phophatidylcholines. *Proc. Natl. Acad. Sci. USA.* 76:15–18.
57. Cullis, P. R. 1976. Hydrocarbon phase transitions, heterogeneous distributions and lipid-protein interactions in erythrocyte membranes. *FEBS (Fed. Eur. Biochem. Soc.) Lett.* 68:173–176.
58. Verma, S. P., and D. F. H. Wallach. 1976. Erythrocyte membranes undergo cooperative, pH-sensitive state transitions in the physiological temperature range: evidence from Raman spectroscopy. *Proc. Natl. Acad. Sci. USA.* 73:3558–3561.
59. Verma, S. P., and D. F. H. Wallach. 1976. Multiple thermotropic state transitions in erythrocyte membranes: a laser Raman study of the CH-stretching and acoustical regions. *Biochim. Biophys. Acta.* 436:307–318.
60. Zimmer, G., and H. Schirmer. 1974. Viscosity changes of erythrocyte membrane and membrane lipids at transition temperature. *Biochim. Biophys. Acta.* 345:314–320.
61. Tanaka, K., and D. Ohnishi. 1976. Heterogeneity in the fluidity of intact erythrocyte membrane and its homogenization upon hemolysis. *Biochim. Biophys. Acta.* 426:218–231.
62. Lentz, B. R., D. A. Barrow, and M. Hoechli. 1980. Cholesterol-phosphatidylcholine interactions in multilamellar vesicles. *Biochemistry.* 19:1943–1954.
63. Axelrod, D. 1977. Cell surface heating during fluorescence photobleaching recovery experiments. *Biophys. J.* 18:129–131.
64. Bernstein, S. E. 1980. Inherited hemolytic disease in mice, a review and update. *Lab. Anim. Sci.* 30:197–205.
65. Matheson, D. W., and J. L. Howland. 1974. Erythrocyte deformation in human muscular dystrophy. *Science (Wash. DC).* 184:165–166.
66. Rubasamen, H., P. Barald, and T. Podleski. 1976. A specific decrease of the fluorescence depolarization of perylene in muscle membranes from mice with muscular dystrophy. *Biochim. Biophys. Acta.* 455:767–779.
67. Feinstein, M. B., S. M. Fernandez, and R. I. Sha'afi. 1975. Fluidity of natural membranes and phosphatidylserine and ganglioside dispersions: effects of local anesthetics, cholesterol and protein. *Biochim. Biophys. Acta.* 413:354–370.
68. Tsong, T. Y., M. Greenberg, and M. I. Kanehisa. 1977. Anesthetic action on membrane lipids. *Biochemistry.* 16:3115–3121.
69. Gazitt, Y., A. Loyter, and I. Ohad. 1977. Induction of ATP depletion, intramembrane particle aggregation and exposure of membrane phospholipids in chicken erythrocytes by local anesthetics and tranquilizers. *Biochim. Biophys. Acta.* 471:361–371.
70. Nicolson, G. L., and G. Poste. 1976. Cell shape changes and transmembrane receptor uncoupling induced by tertiary amine local anesthetics. *J. Supramol. Struct.* 5:65–72.
71. Kehry, M., J. Yguerabide, and S. J. Singer. 1977. Fluidity in the membranes of adult and neonatal human erythrocytes. *Science (Wash. DC).* 195:486–487.
72. Kapitulnik, J., M. Tshershedsky and Y. Barenholz. 1979. Fluidity of the rat liver microsomal membrane: increase at birth. *Science (Wash. DC).* 206:843–844.
73. Clarke, M., G. Schatten, D. Mazia, and J. A. Spudich. 1975. Visualization of actin fibers associated with the cell membrane in amoebae of *Dictyostelium discordeum*. *Proc. Natl. Acad. Sci. USA.* 72:1758–1762.
74. Smith, T. C., and C. Levinson. 1975. Direct measurement of the membrane potential of ehrlich ascites tumor cells: lack of effect of valinomycin and ouabain. *J. Membr. Biol.* 23:349–365.